

The soil effect on the seismic behaviour of reinforced concrete buildings

Burak Yön* and Yusuf Calayır^a

Firat University Civil Engineering Department, Elazığ, Turkey

(Received February 28, 2014, Revised July 14, 2014, Accepted July 26, 2014)

Abstract. This paper investigates the soil effect on seismic behaviour of reinforced concrete (RC) buildings by using the spread plastic hinge model which includes material and geometric nonlinearity of the structural members. Therefore, typical reinforced concrete frame buildings are selected and nonlinear dynamic time history analyses and pushover analyses are performed. Three earthquake acceleration records are selected for nonlinear dynamic time history analyses. These records are adjusted to be compatible with the design spectrum defined in Turkish Seismic Code. Interstory drifts and damages of selected buildings are compared according to local soil classes. Also, capacity curves of these buildings are compared with maximum responses obtained from nonlinear dynamic time history analyses. The results show that, soil class influences the seismic behaviour of reinforced concrete buildings, significantly.

Keywords: local soil class; spread plastic hinge; interstory drift; pushover analysis; time history analysis

1. Introduction

Earthquakes caused collapses and human casualties during history. The recent earthquakes such as 1999 Kocaeli 2003 Bingöl 2010 Kovancılar-Elazığ 2011 Van and Simav-Kütahya earthquakes in Turkey 2003 Lefkada in Greece 2005 Pakistan earthquake in Pakistan 2008 Wenchuan earthquake in China and 2009 L'Aquila earthquake in Italy, have shown that loss of life and property continue still. The researchers expressed that, structural deficiencies such as selection of improper structural system, low material quality and strength, poor workmanship are the most important reasons for serious damages (Adalier and Aydingün (2001), Sezen *et al.* (2003), Doğangün (2004), Calayır *et al.* (2012), Bayraktar *et al.* (2013), Yön *et al.* (2013), Giarlelis *et al.* (2011), Kim and Elnashai (2009), Zhao *et al.* (2009), Palermo *et al.* (2014). However, the soil effect is the other one of main reasons of earthquake damages (Galal and Naimi (2008), Jiang *et al.* (2012)). Damages and collapses can increase due to effect of soil which has a complex and layered structure. These damages substantially occur due to liquefaction, faulting and soil amplification. In this paper, damages of reinforced concrete building which arose from soil effect are investigated.

Therefore, pushover and nonlinear dynamic time history analyses of typical reinforced concrete buildings are performed. For nonlinear dynamic time history analyses, selected earthquake

*Corresponding author, Ph.D., E-mail: burakyon@gmail.com

^aYusuf Calayır, Professor, E-mail: ycalayir@firat.edu.tr

acceleration records are adjusted to be compatible with the design spectrums defined according to local soil classes in Turkish Seismic Code (TSC) (TSC 2007). Interstory drifts and damages of selected buildings are compared according to local soil classes. Also, capacity curves of the selected buildings are compared with maximum responses obtained from nonlinear dynamic time history analyses. In nonlinear analyses, spread plastic hinge approach is used.

2. Modelling approach

The spread plastic hinge approach (fiber element model) accounts distributed plasticity along to the element cross-section and the element length. In this model, the structural element is divided in three types of fibers: some fibers are used for modelling of longitudinal steel reinforcing bars; some of fibers are used to define nonlinear behaviour of confined concrete which consists of core concrete; and other fibers are defined for unconfined concrete which includes cover concrete. Also, for each fiber, the stress/strain field is determined in the nonlinear range by using $\sigma - \varepsilon$ constitutive laws according to defined materials. Fig. 1 shows fiber modelling of a typical fiber model section of a RC element.

This hinge model is more accurate than the point hinge models, especially when large axial force variations exist (Mwafy and Elnashai (2001)). For this reason this model is used by researchers. Dides and Llera (2005) compared plasticity models which include fiber hinge model in dynamic analysis of buildings. Mwafy (2011) assessed seismic design response factors of concrete wall buildings. For this study, five reference structures were selected which their height varying from 20 to 60 stories. Analyses of these structures were performed according to fiber hinge modelling. Duan and Hueste (2012) investigated the earthquake behaviour of a five story reinforced concrete building which designed according to the requirements of the Chinese seismic code. They used fiber hinge model for analyses. Kwon and Kim (2010) assessed a reinforced concrete building which damaged during the 2007 Pisco-Chincha earthquake in Peru.

They performed nonlinear analysis of this building by considering spread hinge model. Kadid *et al.* (2010) investigated behaviour of reinforced concrete buildings under simultaneous ground motions by considering fiber hinge model. Sarno and Manfredi (2010) performed pushover and dynamic analyses for both constructed and retrofitted buildings to investigate the efficiency of buckling restrained braces.

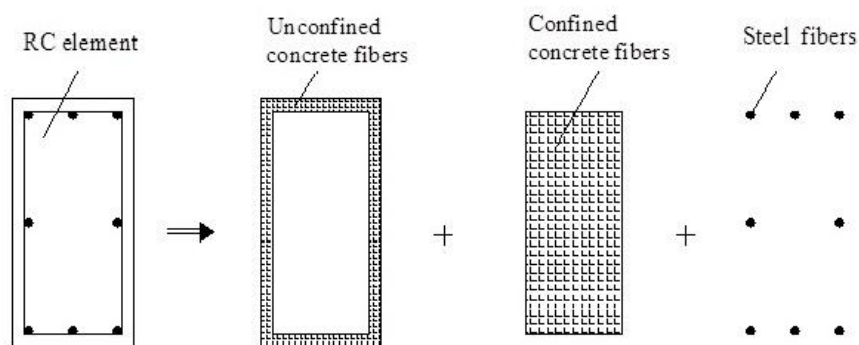


Fig. 1 Typical fiber models of a RC element

They used fiber element model in nonlinear analysis. Yön and Calayır (2013) performed pushover analysis of a reinforced concrete building using lumped and distributed hinge models together with various lateral load patterns. Carvalho *et al.* (2013) investigated comparison of various hinge model approaches by performing nonlinear static and dynamic analysis of a reinforced concrete structure.

In this study, to investigate the soil effect, two reinforced concrete frame buildings are selected. Pushover and nonlinear dynamic time history analyses of these buildings are performed by considering local soil classes named as Z1, Z2, Z3 and Z4 defined in TSC. Spread hinge model is used in nonlinear analyses. Interstory drifts, damages of structural elements, capacity curves of the buildings and maximum responses obtained from nonlinear dynamic time history analyses are compared with each other, by considering local site class. For nonlinear analyses SeismoStruct (SeismoStruct Version 6) program which can simulate the inelastic response of structural systems subjected to static and dynamic loads is used. Also, to scale earthquake acceleration records to design spectrums SeismoArtif (SeismoArtif Version 1.0.0) program is used.

3. The studied buildings and the input

For numerical study, typical high ductility, 5 and 7-storey with 3 bays reinforced concrete frame buildings are selected. The total heights of the buildings are 16.5 and 22.5 m, respectively. The first story heights of the buildings are 4.5 m and the upper story heights are 3.0 m. The dimensions are selected as 60×60 cm for columns, 30×60 cm for beams and 12 cm for the slab thickness. It is assumed that, the buildings are located in high seismic intensity region (seismic zone 1 according to TSC) and have building importance coefficient of 1.0. In the seismic zone map of Turkey, the first seismic zone has 0.4g peak ground acceleration. Concrete compressive strength and yield strength of reinforcing bar are selected as 25 N/mm² and 420 N/mm², respectively. The plan and elevation of the buildings and the cross sections of the structural elements are given in Figs. 2 and 3, respectively. In the buildings; walls which modelled through distributed loads, superimposed dead load and the live load required by the Turkish Standard 498 (TS 498-Design Loads for Buildings) are taken as 2.0 kN/m², 1.5 kN/m² and 2.0 kN/m², respectively. The fundamental periods of 5 and 7-storey buildings determined from SeismoStruct program are 0.596 s and 0.827 s, respectively.

The bilinear elastic plastic material model which includes kinematic strain hardening is used for the reinforcing bar. Concrete material is defined by the uniaxial confinement concrete model (Fig 4) (Kwon and Kim 2010; Duan and Hueste 2012). The confinement effect is calculated by using Mander model (Mander *et al.* 1988). Parameters relating to the confinement zones in structural elements are presented in Table 1. Four Gauss integration points are selected to calculate the element forces and the stress–strain relationship for monitoring each section.

Failure criteria

Seismic performance criteria are based on TSC. Three damage limit levels [Minimum Damage Limit (MN), Safety Damage Limit (GV) and Collapse Damage Limit (GC)] as defined in TSC are used for seismic evaluation. These limit values and colour scale for presentation of structural damages are shown in Tables 2 and 3, respectively.

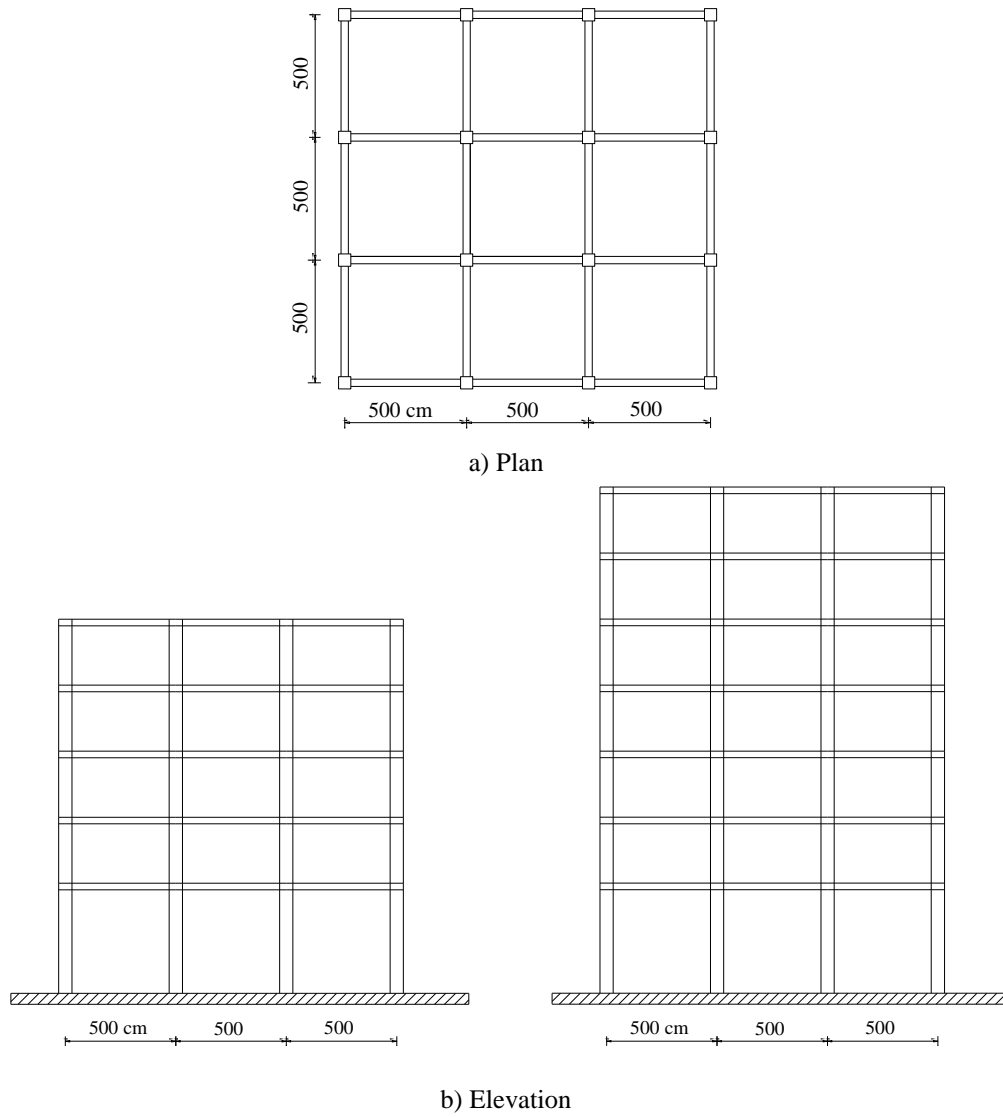


Fig. 2 Plan and elevation of the selected buildings

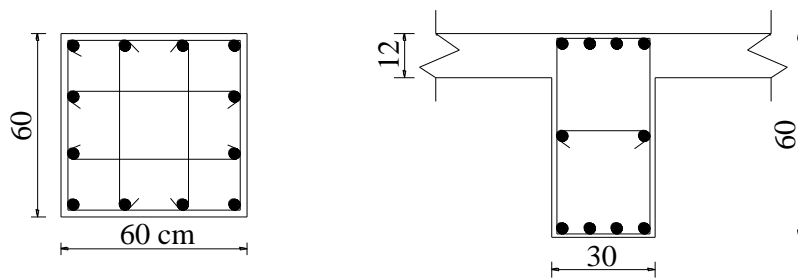


Fig. 3 Column and Beam cross sections

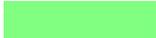
Table 1 Parameters related to the confinement zones in structural elements

	Transverse reinforcement spacing (cm)	Length of confinement zone (cm)	Confinement factor
Confinement zone of column	10	60	1.2597
Central zone of column	15		1.1591
Longitudinal reinforcement of column		12∅ 20	
Confinement zone of beam	10	120	1.1272
Central zone of beam	15		1.0725
Longitudinal reinforcement of beam		4∅ 14-4∅ 14	
Web reinforcement		2x1∅ 14	
Diameter of transverse reinforcement		8 mm	

Table 2 Performance criteria used in determination of damages for structural elements

Damage Level	Limit Values for Confined Concrete	Limit Values for Unconfined Concrete	Limit Values for Steel Bar
Minimum Damage Limit (MN)	$(\epsilon_{cu})_{MN}=0.0035$	0.0035	$(\epsilon_s)_{MN}=0.010$
Safety Damage Limit (GV)	$(\epsilon_{cg})_{GV} = 0.0035 + 0.01(\rho_s/\rho_{sm}) \leq 0.0135$	0.0035	$(\epsilon_s)_{GV}=0.040$
Collapse Damage Limit (GC)	$(\epsilon_{cg})_{GC} = 0.004 + 0.014(\rho_s/\rho_{sm}) \leq 0.018$	0.0040	$(\epsilon_s)_{GC}=0.060$

Table 3 Colour scale used in presentation of structural damage

Damage Boundary	Confined Concrete	Unconfined Concrete	Reinforcing Bar
Minimum Damage Limit			
Safety Damage Limit			
Collapse Damage Limit			

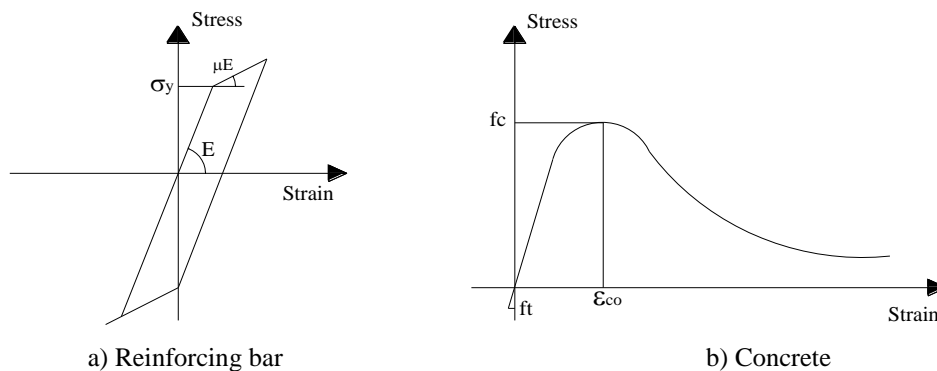


Fig. 4 Material models for reinforcing bar and concrete

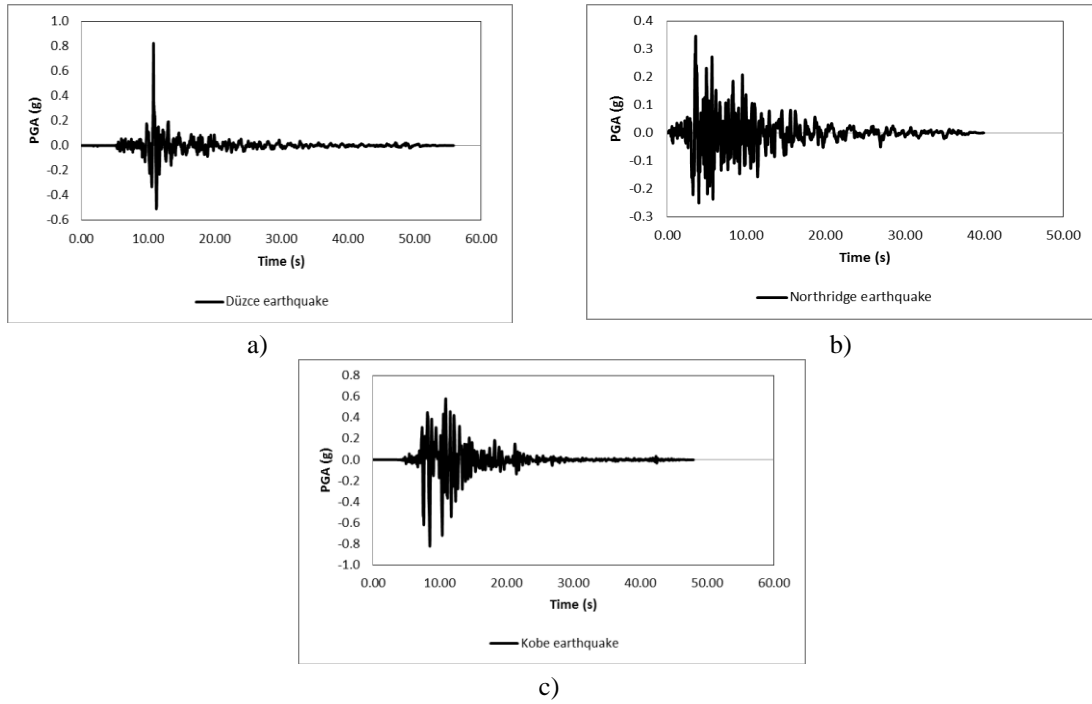


Fig. 5 Earthquake acceleration records used in nonlinear dynamic time history analyses

Table 4 Selected earthquake acceleration records for dynamic analysis

Earthquakes	Station	Direction	Date	Magnitude	PGA (g)	Duration (s)
Düzce	Bolu	East-West	12.11.1999	7.1	0.822	55.89
Northridge	Arleta	East-West	17.01.1994	6.7	0.344	39.98
Kobe	Kjm	North-South	16.01.1995	6.9	0.821	47.98

Table 5 Spectrum characteristic periods according to the soil classes in TSC

Local site classes	T_A (s)	T_B (s)
Z1	0.10	0.30
Z2	0.15	0.40
Z3	0.15	0.60
Z4	0.20	0.90

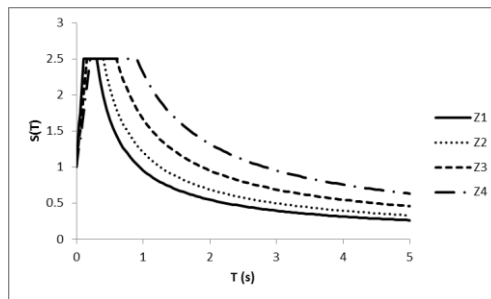
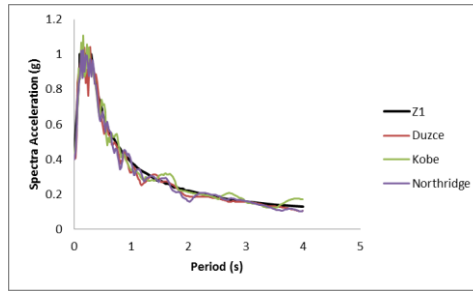
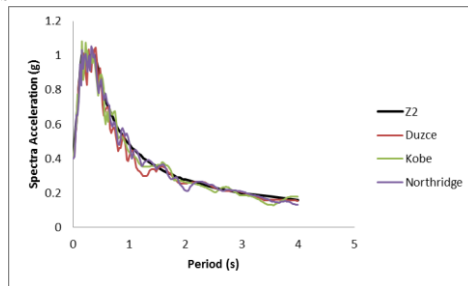


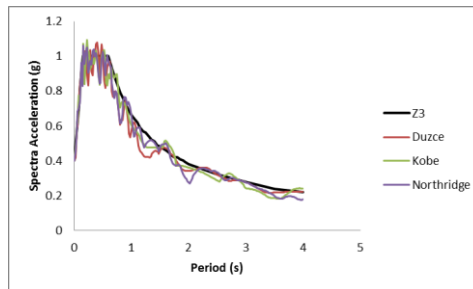
Fig. 6 Design spectra plotted according to four soil classes defined in TSC



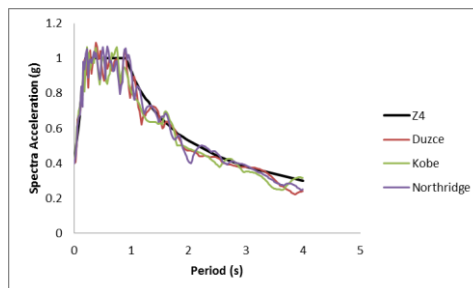
a) Response spectra of the earthquake acceleration records scaled as regards the elastic design spectrum for Z1 soil class



b) Response spectra of the earthquake acceleration records scaled as regards the elastic design spectrum for Z2 soil class



c) Response spectra of the earthquake acceleration records scaled as regards the elastic design spectrum for Z3 soil class



d) Response spectra of the earthquake acceleration records scaled as regards the elastic design spectrum for Z4 soil class

Fig. 7 Response spectra of the earthquake acceleration records scaled as regards the elastic design spectrum for four soil classes defined in TSC

In Table 2, ε_{cu} shows ultimate strain of unconfined concrete while ε_{cg} illustrates ultimate strain of confined concrete. Also, ε_s represents deformation of reinforcement steel unit. ρ_s and ρ_{sm} define volumetric ratio of spiral reinforcement which exist in the cross section and arranged as “special seismic hoops and crossties” and volumetric ratio of the transverse reinforcement necessary to be existed in the cross section, respectively.

The main characteristics of selected earthquake accelerations and graphs are given in Table 4 and Fig. 5, respectively. The seismic records have been selected from the PEER Strong Motion Database and scaled in order to be compatible with the design spectrum by considering four soil classes in TSC.

Soil classes (from Z1 to Z4) are characterized in term of periods T_A and T_B (Table 5) and the design spectrums which plotted according to these soil classes are given in Fig 6.

The selected earthquake records have been scaled both in amplitude and frequency content in order to be compatible with the target design spectrum of four different soil classes (Fig. 7a-d). Thus, effect of softening at soil to the structure behaviour will have been taken into consideration in this way.

4. Results of the numerical analyses

The interstory drifts obtained from the nonlinear dynamic time history analyses for the 5 and 7-storey buildings according to each scaled earthquake acceleration records and soil classes are presented in Figs. 8 and 9.

According to obtained interstory drifts, it is seen that, softening of soil (from Z1 to Z4) causes more displacement demand for structural systems. Especially the Z3 and Z4 soil classes forces the buildings 2-3 times more than the Z1 and Z2 soil classes.

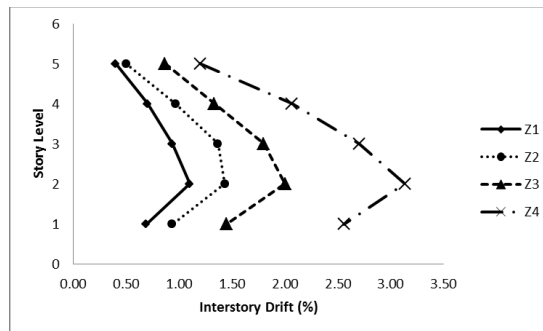
Damage situations for the 5-storey building, obtained from the nonlinear dynamic time history analyses of scaled Düzce earthquake acceleration record are shown in Fig. 10.

According to Fig. 10, damages of the 5-storey building obtained from scaled Düzce earthquake occur only in cover concrete of lower ends of ground floor columns and beam ends for Z1 and Z2 soil classes. For Z3 soil class, core concrete of a lower end of ground floor column damages at safety damage limit. Minimum damages occur in reinforcing bar of the ends of six beams and two columns. However, cover concrete of the ends of five beams and lower end of a column damage at collapse damage limit. For Z4 soil class, while the damage in core concrete reaches to the collapse damage limit at two lower ground column ends, the damage remain at the safety limit in the core concrete of the lower end of a ground floor column. Damages occur at the safety damage limit at the ends of five beams.

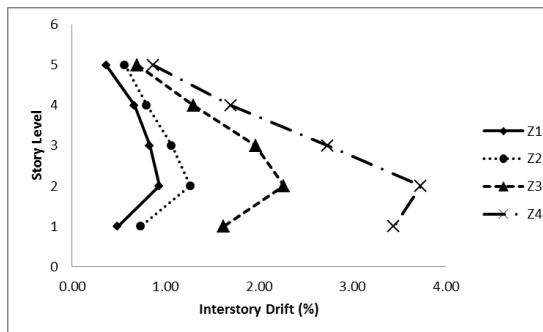
The damage situations for the 5-storey building obtained from scaled Northridge earthquake is given in Fig.11 for four soil classes. Damages occur at collapse damage limit in the cover concrete of almost all beam ends at first, second and third floors for Z1 soil class. There is no damage occurs at columns. Cover concrete of the ends of all beams and lower ends of ground floor columns damage at collapse damage limit for Z2 soil class. Core concrete of lower ends of two ground floor columns damages at safety damage limit for Z3 soil class. Also, cover concrete of lower end of a ground floor column and reinforcing bar of the other column damage at collapse damage limit and minimum damage limit, respectively. However, reinforcing bar damages occur at minimum damage limit at the beam ends of the first and second floors. As for the class Z4,

damages in core concrete of lower ends of ground floor columns reach to collapse and safety damage limits. Core concrete of all beams at the first and second floors damage at safety damage limit and collapse damage limit.

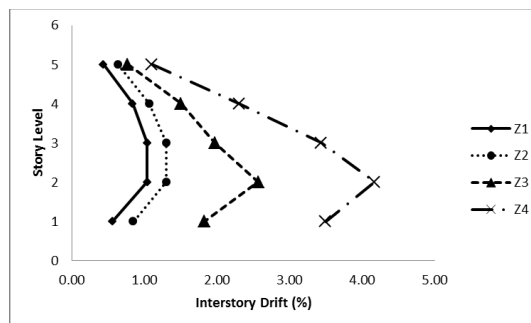
Fig. 12 shows damage situations of the 5-storey building obtained from scaled Kobe earthquake for four soil classes. It is seen that from this figure, damages occur at collapse damage limit in cover concrete of lower ends of three ground floor columns and beam ends of the first and second



a) Düzce earthquake

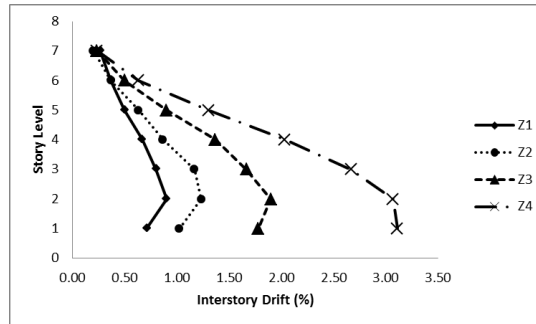


b) Northridge earthquake

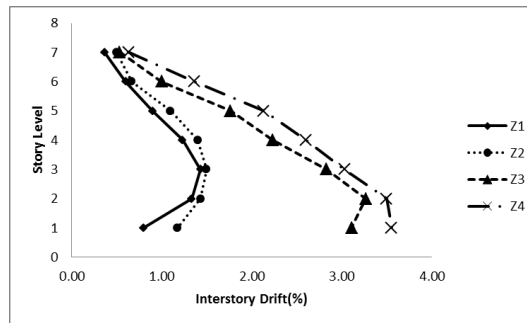


c) Kobe earthquake

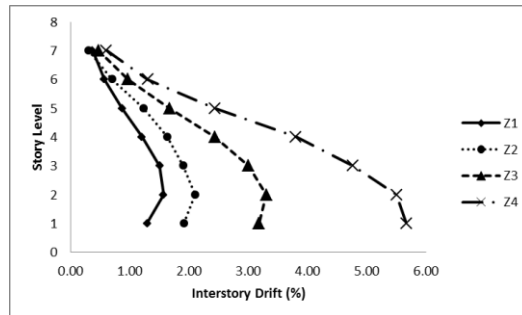
Fig. 8 Interstory drifts of the 5-storey building obtained from the scaled earthquake acceleration records



a) Düzce earthquake



b) Northridge earthquake



c) Kobe earthquake

Fig. 9 Interstory drifts of the 7-storey building obtained from the scaled earthquake acceleration records

floors for Z1 soil class. Damages occur at collapse damage limit in cover concrete of lower ends of the three ground floor columns while minimum damage occurs in reinforcing bar of a column end for Z2 soil class. However, cover concrete of beam ends of the first, second and third floors damage at collapsing damage limit. For Z3 soil class, the damages passed over from cover concrete to core concrete at ground floors and core concrete of lower end of a ground floor column damages at collapsing damage limit. Also, damages occur at safety damage limit at the beam ends of the first floor. For Z4 soil class, core concrete of lower ends of all ground floor columns, and core concrete of beam ends of the first and second floors damage at collapse damage limit.

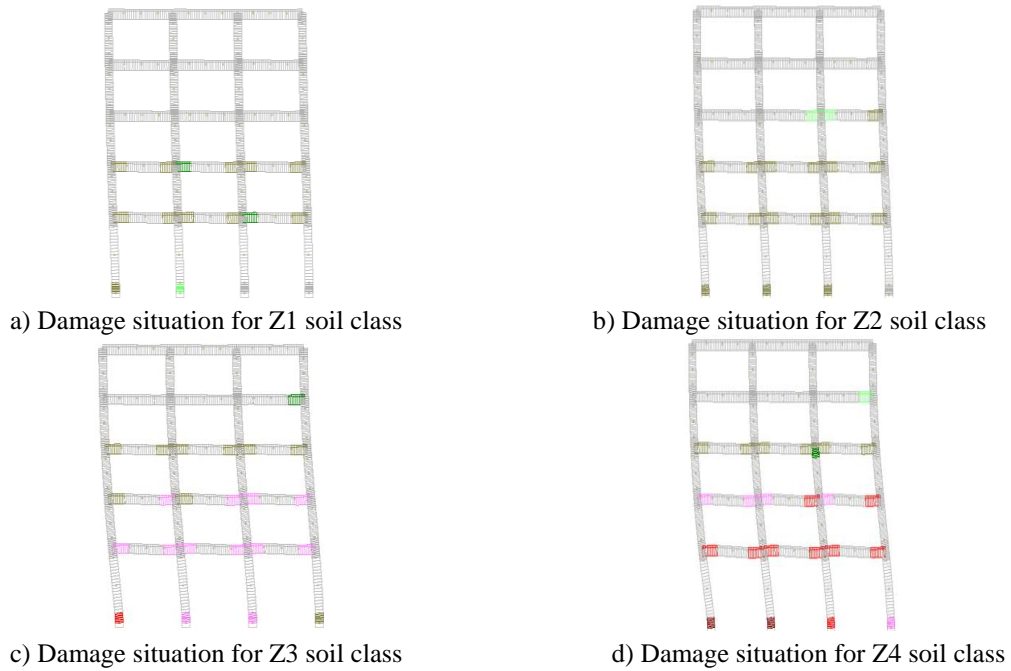


Fig. 10 Damage situations of the 5-storey building obtained from scaled Düzce earthquake acceleration record for various soil classes

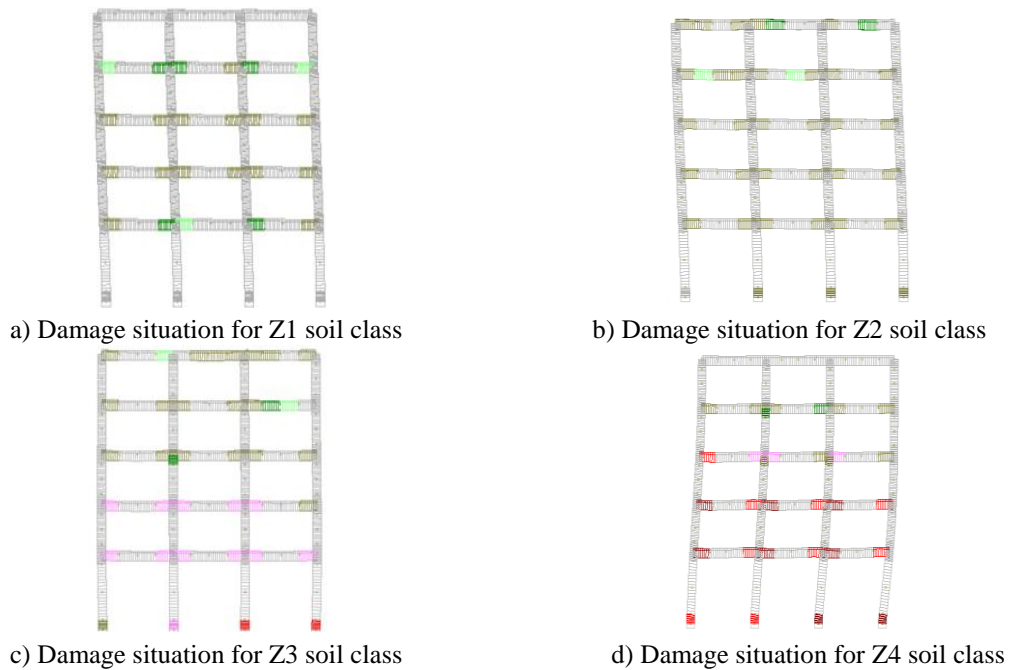


Fig. 11 Damage situations of the 5-storey building obtained from scaled Northridge earthquake acceleration record for various soil classes

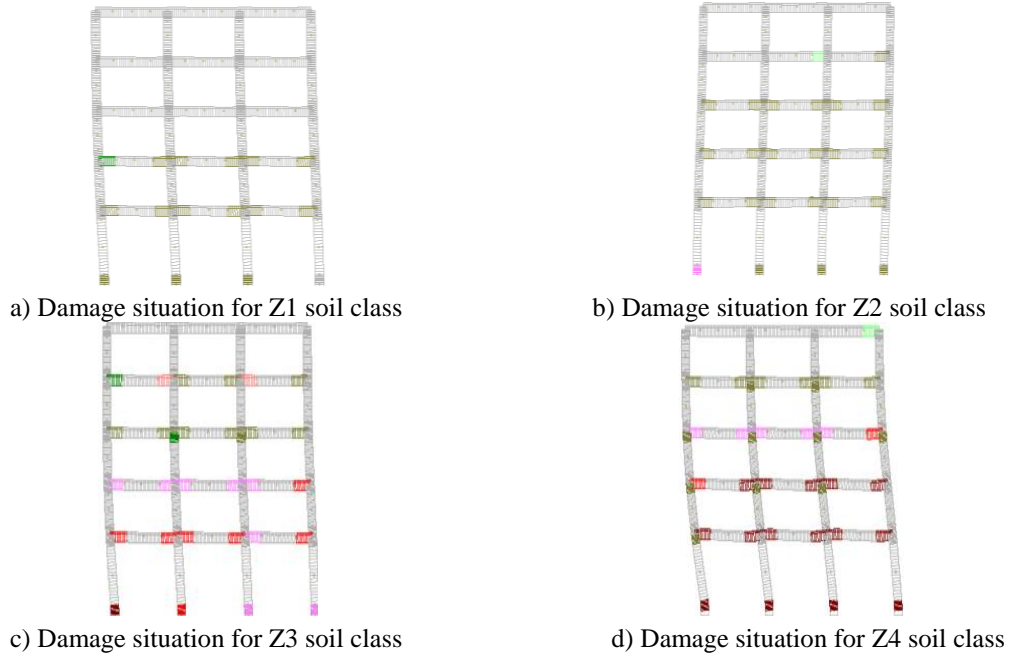


Fig. 12 Damage situations of the 5-storey building obtained from scaled Kobe earthquake acceleration record for various soil classes

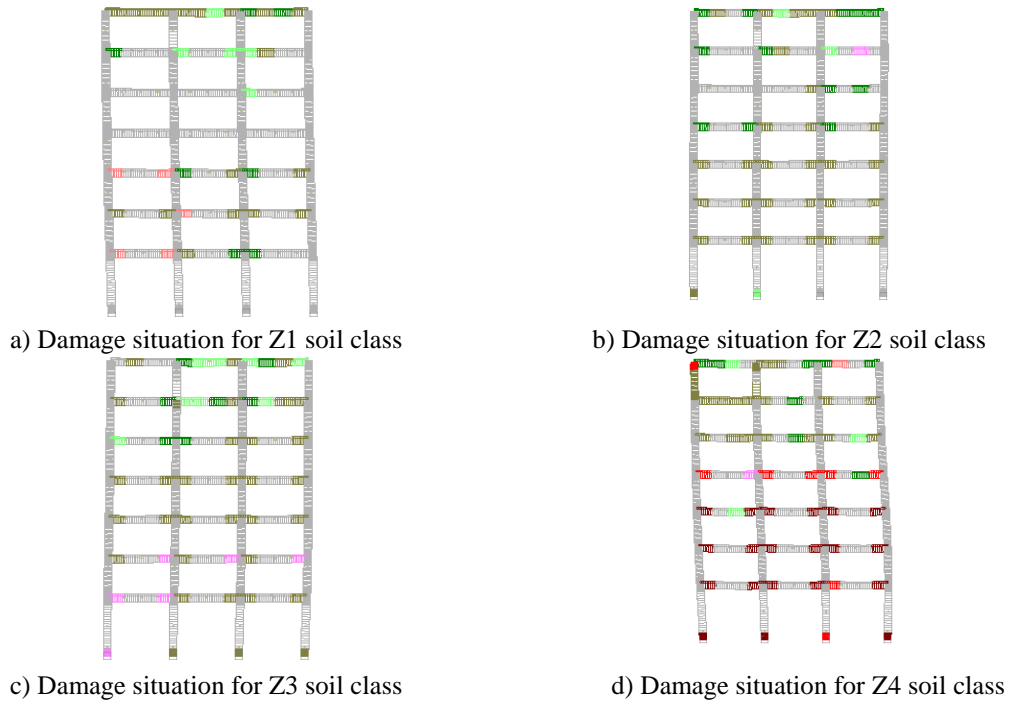


Fig. 13 Damage situations of the 7-storey building obtained from scaled Düzce earthquake acceleration record for various soil classes

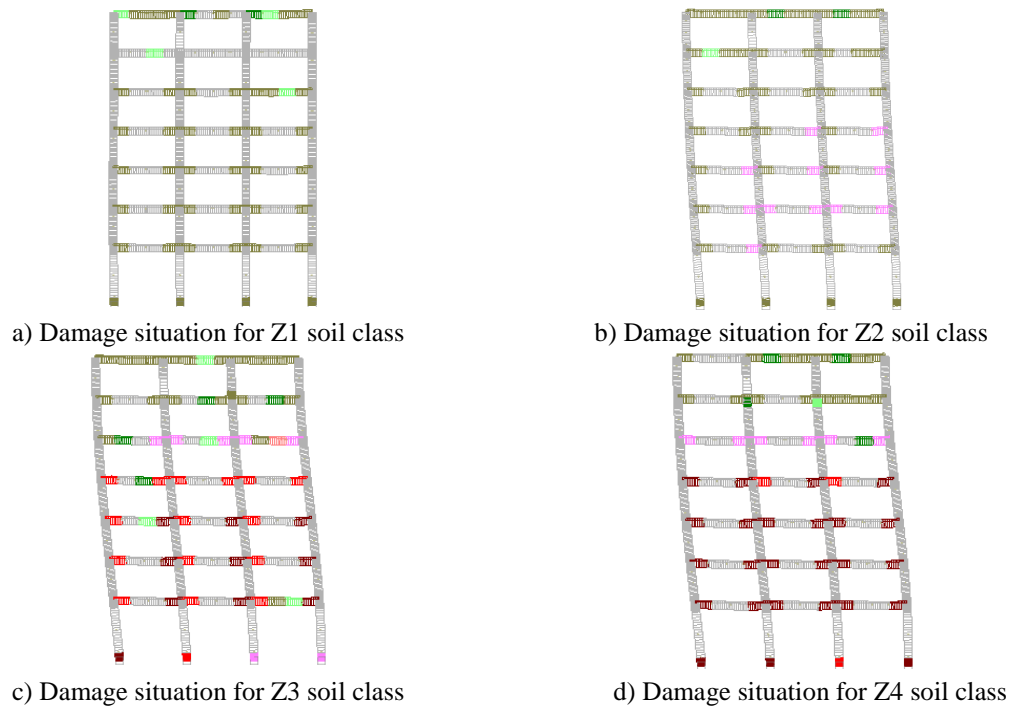


Fig. 14 Damage situations of the 7-storey building obtained from scaled Northridge earthquake acceleration record for various soil classes

Damage situations of the 7-storey building, obtained from nonlinear dynamic time history analyses performed by using scaled Düzce earthquake acceleration record are shown in Fig. 13.

For Z1 soil class there is no damage at the columns of the 7-storey building. Damages occur generally in the cover concrete of beams while minimum damages occur in core concrete of the ends of three beams. For Z2 soil class, damages occur at minimum damage limit and safety damage limit in cover concrete of the lower ends of the ground floor columns. However damages occur in cover concrete of beam ends at safety and collapse damage limit. For Z3 soil class while damage occurs in cover concrete of the lower ends of the three ground floor columns, damage occurs at minimum damage limit in reinforcing bar at the lower end of a column of the ground floor. Except four beams, cover concrete of almost ends of all beams damage at collapse damage limit. For Z4 soil class, while the damage in core concrete reaches to the collapse damage limit at lower ends of the three ground columns, where the most serious damage occurs, the damage remains at the safety limit at the lower end of a column. Damages occur at the collapse damage limit at almost all beam ends of the first, second and third storeys.

The damage situations of the 7-storey building obtained from scaled Northridge earthquake is given in Fig.14 for four soil classes. Damages occur at collapse damage limit in the cover concrete of almost all beam ends and the lower ends of ground floor columns for Z1 soil class.

For Z2 soil class, the reinforcing bar damages occur at minimum damage limit at the ends of nine beams while the cover concrete of the ends of other beams and lower ends of the ground floor columns damage at collapse damage limit. For Z3 soil class, core concrete of lower end of the column damage at collapse damage limit, damage of the other column end reaches to the safety

damage limit, and reinforcing bar of the lower ends of the other two columns reach to minimum damage limit. At lower floors, core concrete of beam ends damage at safety and collapse damage limits. As for the class Z4, damages at core concrete of lower ends of ground floor columns reaches to collapse and safety damage limits. However, core concrete of almost all beams at the lower floors damage at collapse damage limit.

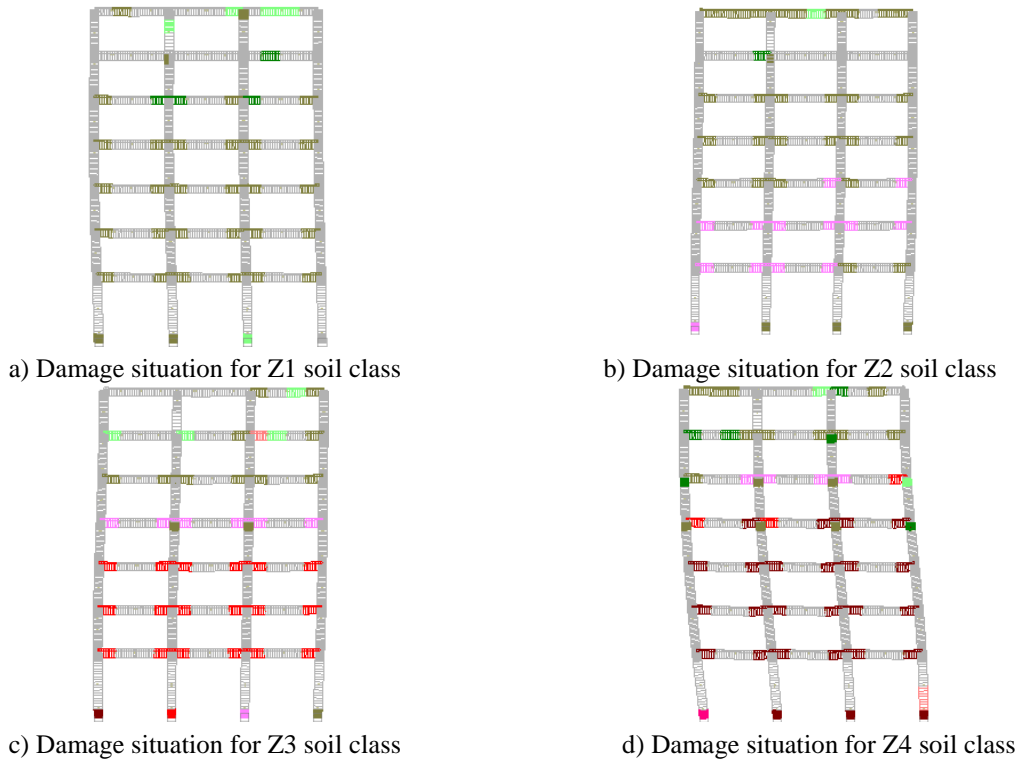


Fig. 15 Damage situations of the 7-storey building obtained from scaled Kobe earthquake acceleration record for various soil classes

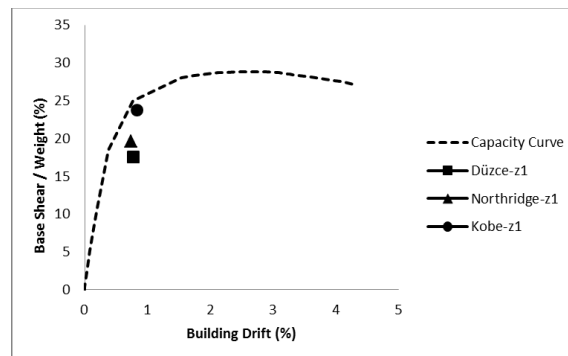


Fig. 16 Comparison of the dynamic time history analyses results and the capacity curve of the 5-storey building for Z1 soil class

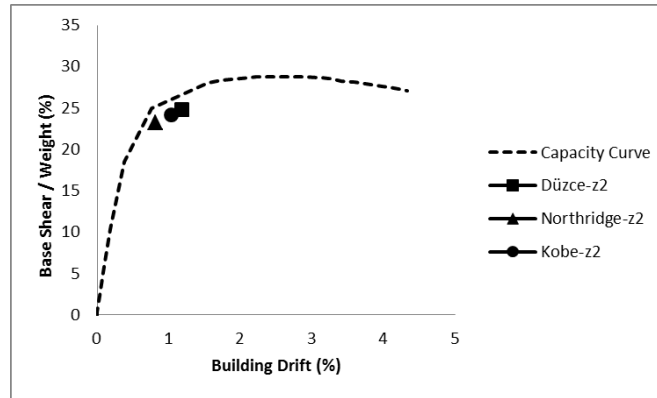


Fig. 17 Comparison of the dynamic time history analyses results and the capacity curve of the 5-storey building for Z2 soil class

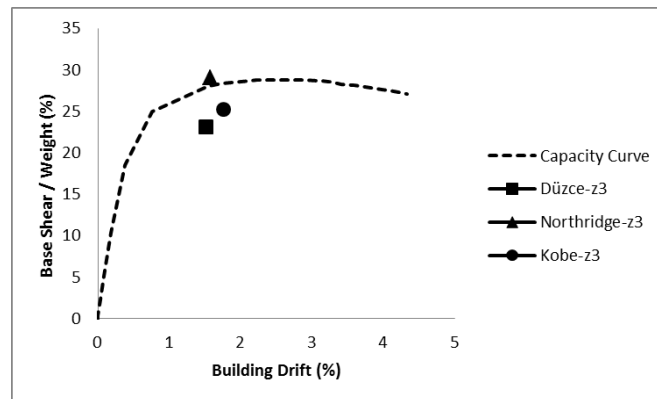


Fig. 18 Comparison of the dynamic time history analyses results and the capacity curve of the 5-storey building for Z3 soil class

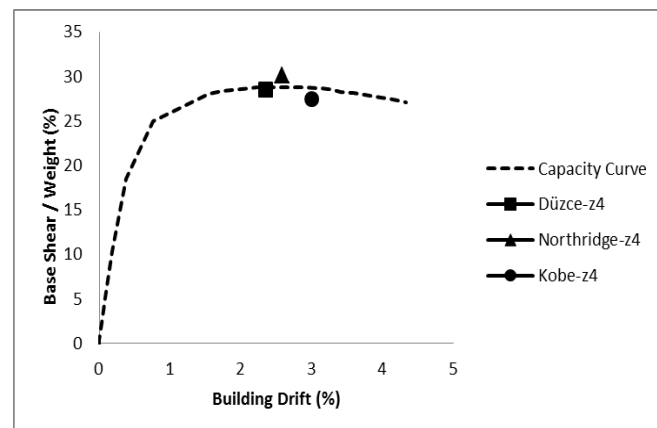


Fig. 19 Comparison of the dynamic time history analyses results and the capacity curve of the 5-storey building for Z4 soil class

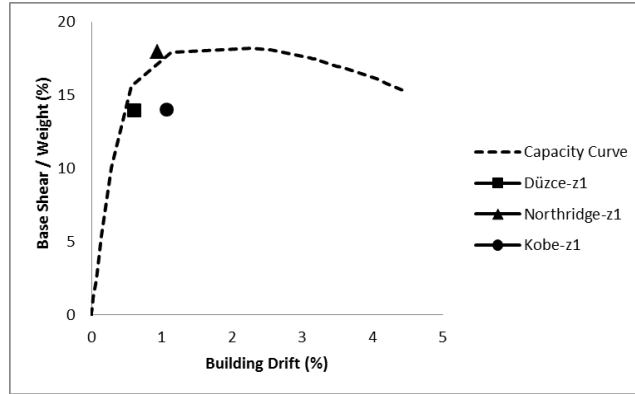


Fig. 20 Comparison of the dynamic time history analyses results and the capacity curve of the 7-storey building for Z1 soil class

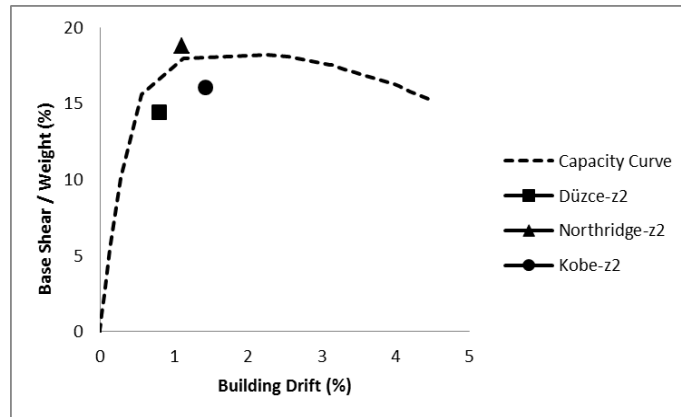


Fig. 21 Comparison of the dynamic time history analyses results and the capacity curve of the 7-storey building for Z2 soil class

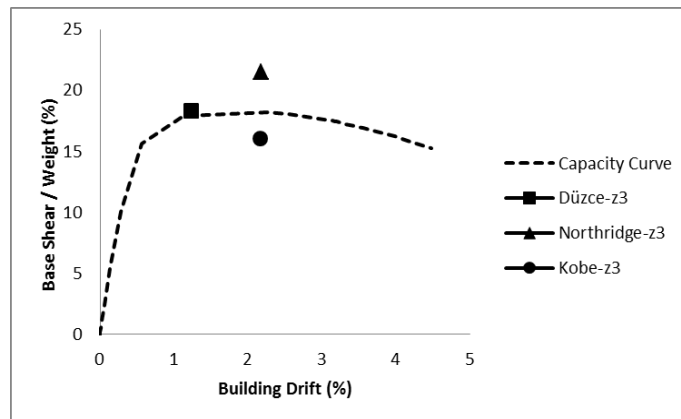


Fig. 22 Comparison of the dynamic time history analyses results and the capacity curve of the 7-storey building for Z3 soil class

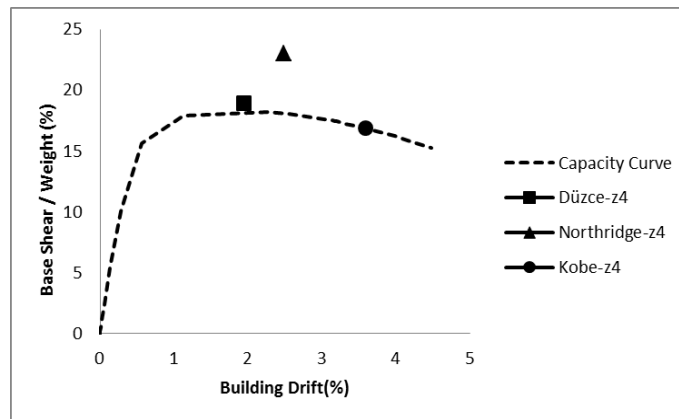


Fig. 23 Comparison of the dynamic time history analyses results and the capacity curve of the 7-storey building for Z4 soil class

The damage situations of the 7-storey building obtained from scaled Kobe earthquake are presented in Fig.15 for four soil classes. While damage occurs at collapse damage limit in cover concrete of lower ends of two ground floor columns for Z1 soil class, damage occurs at safety damage limit in cover concrete of lower end of a ground floor column. However, damage occurs at collapse damage limit in cover concrete of all beam ends of the first four floors. For Z2 soil class damage occurs in cover concrete of lower ends of three ground floor columns while minimum damage occurs in reinforcing bar of a column end. With regards to beams, damage of the reinforcing bar reaches to minimum damage limit at ends of seven beams of the first three stories. Also, damages occur at collapse damage limit in cover concrete of the other beam ends. For Z3 soil class, the damages pass over from cover concrete to core concrete at ground floors and damages occur at safety limit at the beam ends of the first three floors. Also, damages occur in core concrete of lower ends of the ground floor columns at collapse and safety damage limits, respectively. Minimum damages occur in reinforcing bars and cover concrete of the other lower ends of the ground floor columns damage at collapse damage limit. For Z4 soil class, damages occur at collapse damage limit in core concrete of the lower ends of three ground floor columns and beam ends of the first four floors. However, damage of reinforcing bar reaches to the safety limit at central zone of a column. It is seen from the damage situations of the buildings, softening of soil increase damages, significantly.

Figs. 16-19 shows, comparison of maximum responses of the dynamic analyses obtained from scaled records according to each soil class and capacity curve of the selected 5-storey building.

According to Fig. 16; the maximum responses obtained from Düzce, Kobe and Northridge earthquakes remain under the capacity curve of the 5-storey building for Z1 soil class. Also, it is determined that, the building drifts for the same soil class are at a level of 1% for each three earthquakes. It is seen from Fig.17; the building drifts are between 1% and 1.5% for Z2 soil class and maximum responses of all earthquakes remain under the capacity curve. As for the soil class Z3, it is seen from Fig. 18; maximum response of Northridge earthquake exceeds the capacity curve of building at nearly 2% building drift level. It is determined from Fig. 19; the maximum responses of Düzce and Northridge earthquakes exceed the capacity curve for Z4 soil class.

Figs. 20-23 shows, comparison of maximum responses of the dynamic analyses obtained from

scaled records according to each soil class and capacity curve of the selected 7-storey building.

It is seen from Fig. 20; for Z1 soil class the maximum responses of the Düzce and Kobe earthquakes remain under the capacity curve of the building. However, the maximum response of the Northridge earthquake takes place just above the capacity curve. Also, it is determined that, the building drifts for each three earthquakes are at a level of 1% for Z1 soil class. According to Fig. 21; for Z2 soil class, the building drifts for all earthquakes are between 1% and 2% and results are similar to Z1 soil class. As for the soil class Z3, it is seen from Fig. 22; maximum responses of the Northridge and Düzce records exceed the capacity curve of the building. It is determined from Fig. 23; maximum responses of all the earthquakes exceed the capacity curve of the building for Z4 soil class. These results clearly show that, the soil effect influences the building drifts, significantly.

5. Conclusions

In this study, the effect of soil class on seismic behaviour of reinforced concrete buildings is evaluated by using spread plastic hinge approach. Therefore, pushover and nonlinear dynamic time history analyses of two typical reinforced concrete frame buildings are performed by using earthquake acceleration records (1999 Düzce 1995 Kobe and 1994 Northridge) which scaled design spectrum defined in Turkish Seismic Code. Interstory drifts and damages at selected buildings are compared according to local soil classes. Also, capacity curves of the selected buildings are compared with maximum responses obtained from nonlinear dynamic time history analyses.

The interstory drifts are show that, increasing of soil class from Z1 to Z4, causes more displacement demand at structural systems. It is seen that, especially the Z3 and Z4 soil classes force the buildings 2-3 times more than the other soil classes.

According to scaled Düzce earthquake, for Z1 soil class, damages both 5 and 7-storey buildings occur in cover concrete of beams and columns. But at 7-storey building, core concrete of some beams damage at minimum damage limit. For Z2 soil class, although damages occur in cover concrete of beams and columns at 5 and 7-storey buildings, more beams and columns damage than Z1 soil class. For Z3 soil class, damages of 7-storey building occur in cover concrete and reinforcing bar of beams and columns at collapse damage limit and minimum damage limit. However, for 5-storey buildings, damages at beams and columns occur in core concrete, cover concrete and reinforcing bar at safety damage, collapse damage and minimum damage limits, respectively. For Z4 soil class, damages at core concrete of beam and column ends of 5 and 7-storey buildings reach to collapse damage limit.

According to scaled Northridge earthquake, for Z1 soil class, both 5 and 7-storey buildings damages occur at collapse damage limit in the cover concrete of almost all beam ends. However, at 7-storey building damages occur in the cover concrete of column ends. For 7-storey building the reinforcing bars of some beams damages at minimum damage limit for Z2 soil class. Damages at 5-storey building occur in cover concrete of beams and columns. However, for Z3 soil class, damages of both 5 and 7-storey buildings occur in core concrete of lower end of columns at safety and collapse damage limits, respectively. Damages at beams of the 7-storey building occur in core concrete of lower floor beams at safety and collapse damage limits. But at 5-storey building less damage occurs than the other building. For Z4 soil class, core concrete of beams and column ends

of both 5 and 7-storey buildings damage at collapse damage limit.

In terms of scaled Kobe earthquake, for Z1 soil class, cover concrete of beams and column ends of both 5 and 7-storey buildings damage at collapse damage limit. For Z2 soil class, damage occurs in cover concrete at collapse damage limit while minimum damage occurs in reinforcing bar of 5 and 7-storey buildings. For Z3 soil class, damages at beams and columns ends occur at safety and collapse damage limits at both 5 and 7 storeys buildings. For Z4 soil class, damages occur in core concrete at collapse damage limit for two buildings.

For 5-storey building, the maximum responses obtained from scaled earthquake records remain under the capacity curve of the building for Z1 and Z2 soil class. As for the soil class Z3, maximum response of the scaled Northridge earthquake exceeds the capacity curve. The maximum responses of Düzce and Northridge earthquakes exceed the capacity curve for Z4 soil class. According to Z1 soil class, for 7-storey building, the maximum responses of the Düzce and Kobe earthquakes remain under the capacity curve of the building. However, the maximum response of the Northridge earthquake takes place just above the capacity curve. For Z2 soil class, results are similar to Z1 soil class. As for the soil class Z3, maximum responses of the Northridge and Düzce exceed the capacity curve of the building. For Z4 soil class, maximum responses of all earthquakes exceed the capacity curve of building. These results clearly show that, the soil class influences the building drifts, significantly.

It is seen that, increasing of soil class from Z1 to Z4 enhances interstorey drifts, damages at structural elements and building drifts. Also, it is determined that, increase of storey number enhances the damages. This results show that, soil has important factor for seismic behaviour of buildings. For this reason, when buildings are designed and constructed, the soil effect should be considered.

Acknowledgments

The authors gratefully thank to Seismosoft for providing free license for SeismoStruct and SeismoArtif software.

References

- Adalier, K. and Aydingün, O. (2001), "Structural engineering aspects of the June 27, 1998 Adana–Ceyhan (Turkey) earthquake", *Eng. Struct.*, **23**, 343-355.
- Bayraktar, A. Altunışık, A.C. and Pehlivan, M. (2013) "Performance and damages of reinforced concrete buildings during the October 23 and November 9, 2011 Van, Turkey, earthquakes" *Soil Dyn. Earthq. Eng.* **53**, 49-72.
- Calayır, Y. Sayın, E. and Yön, B. (2012), "Performance of structures in the rural area during the March 8, 2010 Elazığ-Kovancılar earthquake", *Nat. Hazards*, **61**(2), 703-717.
- Carvalho, G. Bento, R. and Bhatt, C. (2013), "Nonlinear static and dynamic analyses of reinforced concrete buildings – comparison of different modeling approaches", *Earthq. Struct.*, **4** (5), 451-470.
- Dides, M. A. and Llera, J.C.D. (2005), "A comparative study of concentrated plasticity models in dynamic analysis of building structures", *Earthq. Eng. Struct. Dyn.* **34**, 1005-1026.
- Doğangün, A. (2004), "Performance of reinforced concrete buildings during the May 1, 2003 Bingöl earthquake in Turkey", *Eng. Struct.*, **26**(6), 841-856.

- Duan, H. and Hueste, M.B.D. (2012), "Seismic performance of a reinforced concrete frame building in China", *Eng. Struct.* **41**, 77-89.
- Giarlelis, C., Lekka, D., Mylonakis, G. and Karabalis, D.L. (2011), "The M6.4 Lefkada 2003, Greece, earthquake: dynamic response of a 3-storey R/C structure on soft soil", *Earthq. Struct.*, **2**(3), 257-277.
- Galal, K. and Naimi, M. (2008), "Effect of soil conditions on the response of reinforced concrete tall structures to near fault earthquakes", *Struct. Des. Tall Spec. Build.*, **17**, 541-562.
- Jiang, H., Lu, X., and Chen, L. (2012), "Seismic fragility assessment of RC moment-resisting frames designed according to current Chinese seismic design code", *J. Asian Arc. Build. Eng.* **11-1**, 153-160.
- Kadid, A., Yahiaoui, D. and Chebili, R. (2010), "Behaviour of reinforced concrete buildings under simultaneous horizontal and vertical ground motions", *Asian J. Civil Eng. (Building and Housing)*, **11**, 463-476.
- Kim, S.J. and Elnashai, A.S. (2009), "Characterization of shaking intensity distribution and seismic assessment of RC buildings for the Kashmir (Pakistan) earthquake of October 2005", *Eng. Struct.*, **31**, 2998-3015.
- Kwon, O.S. and Kim, E. (2010), "Case study: Analytical investigation on the failure of a two-story RC building damaged during the 2007 Pisco-Chincha earthquake", *Eng. Struct.*, **32**, 1876-1887.
- Mander, J.B., Priestley, M.J.N. and Park, R. (1988), "Theoretical stress-strain model for confined concrete", *J. Struct. Eng.*, 1804-1826.
- Mwafy, A.M. and Elnashai, A.S. (2001), "Static pushover versus dynamic collapse analysis of RC buildings", *Eng. Struct.*, **23**, 407-424.
- Mwafy, A. (2011), "Assessment of seismic design response factors of concrete wall buildings", *Earthq. Eng. Eng. Vib.*, **10**, 115-127.
- PEER Strong Motion Database, www.peer.berkeley.edu/smcat/search.html
- Sarno, L.D. and Manfredi, G. (2010), "Seismic retrofitting with buckling restrained braces: Application to an existing non-ductile RC framed building", *Soil Dyn. Earthq. Eng.*, **30**, 1279-1297.
- Sezen, H. Whittaker, A.S. Elwood, K.J. and Mosalam, K.M. (2003), "Performance of reinforced concrete buildings during the August 17, 1999 Kocaeli, Turkey earthquake, and seismic design and construction practice in Turkey", *Eng. Struct.*, **25**(1), 103-114
- SeismoStruct Version 6 available on www.seismosoft.com
- SeismoArtif Version 1.0.0 available on www.seismosoft.com
- Turkish Seismic Code 2007, Ankara, Turkey
- TS 498 Design Loads for Buildings, Turkish Standards Institute, Ankara, Turkey
- Palermo, M., Hernandez, R.R., Mazzoni, S. and Trombetti, T. (2014), "On the seismic behavior of a reinforced concrete building with masonry infills collapsed during the 2009 L'Aquila earthquake", *Earthq. Struct.*, **6** (1), 45-69.
- Yön, B. Sayın, E. and Köksal, T.S. (2013), "Seismic response of buildings during the May 19, 2011 Simav, Turkey earthquake", *Eartq. Struct.*, **5** (3), 343-357.
- Yön, B. and Calayır, Y. (2013), "Pushover analysis of a reinforced concrete building according to various hinge models", *2nd International Balkans Conference on Challenges of Civil Engineering, BCCCE*, Tirana, Albania 23-25 May.
- Zhao, B. Taucer, F. and Rossetto, T. (2009), "Field investigation on the performance of building structures during the 12 May 2008 Wenchuan earthquake in China", *Eng. Struct.*, **31**, 1707-1723.